Skeleton Extraction via Anisotropic Heat Flow

Cem Direkoglu
cem.direkoglu@scss.tcd.ie
Rozenn Dahyot
rozenn.dahyot@scss.tcd.ie
Michael Manzke
michael.manzke@cs.tcd.ie

School of Computer Science and Statistics,
Trinity College Dublin,
Ireland

Abstract

We introduce a novel skeleton extraction algorithm in binary and gray-scale images, based on the anisotropic heat diffusion analogy. We propose to diffuse image in the dominance of direction normal to the feature boundaries and also allow tangential diffusion to contribute slightly. The proposed anisotropic diffusion provides a high quality medial function in the image, since it removes noise and preserves prominent curvatures of the shape along the level-sets (skeleton locations). Then the skeleton strength map, which provides the likelihood to be a skeleton point, is obtained by computing the mean curvature of level-sets. The overall process is completed by non-maxima suppression and hysteresis thresholding to obtain thin and binary skeleton. Results indicate that this approach has advantages in handling noise in the image and in obtaining smooth shape skeleton because of the directional averaging inherent of our new anisotropic heat flow.

1 Introduction

Skeleton or medial axis [2] is a thin version of the shape, which is an important feature for shape description in image processing and computer vision. It offers simple and compact representation of shapes while preserving its topology. There are different algorithms for skeletonization of shapes in images. We first review techniques which are limited to the pre-segmented binary images and then review techniques that are capable to extract skeletons from gray-scale images.

Popular techniques used for skeleton extraction in binary images are based on thinning [12], Voronoi diagrams [16], distance transform [1] [10] [14], Poisson equation [6], Newton law [17] and Electrostatic field [7]. Thinning [12] is a process that deletes object boundary pixels iteratively with a set of conditions. Complex conditions are required to terminate deleting process as well as to preserve topology and connectivity of the skeleton. In [16], the skeleton is computed from the Voronoi diagram of a set points on the boundary of the object. This approach is theoretically well defined in a continuous space, which means high sampling rate of the boundary points are required to obtain a good quality Voronoi diagram. The Voronoi skeletons also need complex post-processing stages to prune branches. A medial function is a scalar function that locally assigns skeleton points higher

BMVC 2010 doi:10.5244/C.24.61

values than non-skeleton ones. Many techniques [1] [10] [14] use distance transform as a medial function to extract skeletons. The distance transform computes at each shape point its minimum distance to the shape boundary. However, the distance transform is very sensitive to the small perturbations of the boundary, since each value on shape is assigned according to the single boundary point (nearest one). To overcome the limitations of distance transform a few smooth medial functions are introduced which are based on Newton law [17], Electrostatic field [7] and Poisson equation [6]. The values assigned by each function at a point take into account several boundary points and they reflect more global properties than the distance transform. However, all these methods presented above require pre-segmented binary images, since they use object boundary to compute skeletons.

Tari et al. [18] extract skeletons from gray-scale images by analysing the level-set curves of the edge strength function. The edge strength function is computed using the linear diffusion equation. Lindeberg [13] treated the skeletonization in a similar way of edge detection in scale-space [20], with automatic scale selection. Scale-space involves generating coarser resolution images by convolving the original image with a Gaussian kernel. In [11] and [8], it has been pointed out that the family of derived images using Gaussian kernel may be equivalently viewed as the solution of linear heat diffusion equation. According to the linear heat diffusion, blurring is required to be spatially invariant which makes it difficult to obtain accurately the location of edge and skeleton features, at coarse scales. Linear diffusion techniques can cause lose of skeleton features, which is an important drawback. There are also approaches which uses gradient vector diffusion for skeleton extraction in gray-scale images. The first gradient vector diffusion was introduced by Xu and Prince [21] as a new external force model for active contours in the shape extraction context. Then, this model is adapted for skeleton extraction [22] [3]. Yu and Bajaj [22] compute skeletons in gray-level images based on anisotropic gradient vector diffusion, where the initial vector fields are obtained by various ways to overcome noise in images. The gradient-based information is limited by noise as known from the active contour models [5]. Image smoothing or some heuristics [22] can be applied to improve initial gradient vector field. However, they can just increase the tolerance to the noise and they may also lose important features after smoothing.

Given a smooth medial function, the curvature maxima along the level-sets define the shape skeleton [18] [13]. In this paper, we propose a novel medial function, which can be computed both for binary and gray-scale images, based on the anisotropic heat diffusion. We mainly diffuse image in the direction normal to the edges and also allow tangential diffusion (curvature decreasing diffusion) to make small contribution. The proposed heat diffusion denoises image and object boundary, while preserving the prominent curvatures of the shape along the level-sets that represent skeleton locations. After we compute the medial function with the proposed anisotropic diffusion, the skeleton strength map is simply defined by mean curvature measure. Finally, thin and binary skeleton is obtained by non-maxima suppression and hysteresis thresholding to the skeleton strength map. Our technique extracts skeleton better than the techniques based on linear diffusion of images, since they cause curvature shrinkage and lose of skeleton features. We can handle noise and extract smooth shape skeleton in both binary and gray-scale images.

The rest of the paper is organized as follows: Section 2 introduces the proposed anisotropic heat diffusion for a novel medial function generation. Section 3 is experimental results and comparison with other techniques, prior to conclusions.

2 Proposed Diffusion and Skeleton Extraction

In skeleton extraction, it is an important task to compute a smooth and high quality medial function that can provide skeleton features easily and without noise. One of the main features for skeleton point detection is curvature maxima along the level-sets of the medial function. In this section, we present the proposed anisotropic heat diffusion as a novel medial function generation technique, which can remove noise in the image and can preserve the prominent curvatures of the object shape along the level-sets. Note that an introductory tutorial about the heat diffusion equation is also given in [19] [4]. The proposed anisotropic heat diffusion equation is obtained with the following considerations.

Edge directions are related to the tangents of the feature boundaries of an image I. Let η denote the direction normal to the feature boundary through a given point (the gradient direction), and let τ denote the tangent direction. These directions can be written in terms of the first derivatives of the image, I_x and I_y, as

$$\eta = \frac{(I_x, I_y)}{\sqrt{I_x^2 + I_y^2}}, \qquad \tau = \frac{(-I_y, I_x)}{\sqrt{I_x^2 + I_y^2}} \tag{1}$$

Since η and τ constitute orthogonal directions, the rotationally invariant Laplacian operator can be expressed as the sum of the second order spatial derivatives, $I_{\eta\eta}$ and $I_{\tau\tau}$, in these directions and the linear heat conduction equation can be written as follows,

$$\frac{\partial I}{\partial t} = \nabla^2 I = (I_{\eta\eta} + I_{\tau\tau}) \tag{2}$$

Omitting the normal diffusion, while keeping the tangential diffusion yields the well known Geometric Heat Flow (GHF) equation [9] as

$$\frac{\partial I}{\partial t} = I_{\tau\tau} = \frac{(I_{xx} I_y^2 - 2 I_{xy} I_x I_y + I_{yy} I_x^2)}{(I_x^2 + I_y^2)} \tag{3}$$

GHF is an anisotropic diffusion and is widely used for image denoising and enhancement. It diffuses along the boundaries of image features, but not across them. It removes noise in the image and preserves prominent edges. It derives its name from the fact that, under this flow, the feature boundaries of the image evolve in the normal direction in proportion to their curvature. Thus GHF decreases the curvature of level-sets of the image while removing noise to obtain sharp edges.

On the other hand, omitting the tangential diffusion, while keeping the normal diffusion in the heat equation yields

$$\frac{\partial I}{\partial t} = I_{\eta\eta} = \frac{(I_{xx} I_x^2 + 2 I_{xy} I_x I_y + I_{yy} I_y^2)}{(I_x^2 + I_y^2)} \tag{4}$$

Normal diffusion is also an anisotropic diffusion. It diffuses across the edges in the image and do not preserve them. Because of this property, it did not take much attention for image smoothing and enhancement or for edge detection. Significant application of the normal diffusion can only be observed in [15] for image segmentation. In this application, the normal diffusion is called Anti-Geometric Heat Flow (A-GHF), since the diffusion is in orthogonal direction to the GHF.

Here, we choose the normal diffusion as a main tool for medial function generation in binary and gray-scale images for skeleton extraction purpose. The normal diffusion can preserve prominent curvatures of the shapes along the level-sets in images while removing noise, since it does not diffuse along the level-sets (in tangent direction). However, we do not completely omit tangential diffusion and let it contribute slightly depending on the user, since it can also remove noise along the feature boundaries and contribute to obtain smoother skeleton. The proposed anisotropic heat diffusion problem for medial function generation is given below,

$$\begin{aligned} \frac{\partial I}{\partial t} &= I_{\eta\eta} + c\, I_{\tau\tau} \quad , \quad 0 \le c \le 0.4 \\ I(\mathbf{x}, t=0) &= F(\mathbf{x}), \quad \text{initial condition} \\ \frac{\partial I(\mathbf{x},t)}{\partial n} &= 0, \quad \text{boundary condition} \end{aligned} \tag{5}$$

where $0 \le c \le 0.4$ is the diffusion coefficient which is a positive constant and bounded to prevent excess smoothing in direction tangent. Note that in our experiments $c = 0.2$. $\mathbf{x} = (x, y)$ is the space vector and $F(\mathbf{x})$ is the input binary or gray-scale image, which represents initial condition of the diffusion problem. The boundaries of the image are insulated with homogeneous Neuman condition, $dI/dn = 0$, which means there is no heat flow in, or out of the image domain definition. Note that in boundary condition n represents direction normal to the image boundary.

The skeleton strength map is likelihood for each pixel to be a skeleton point. In our algorithm, the skeleton strength map (*SSM*) is the mean curvature measure of the level-sets that is computed after terminating diffusion,

$$SSM = \nabla \cdot \left(\frac{\nabla I(\mathbf{x}, t_s)}{|\nabla I(\mathbf{x}, t_s)|} \right) \tag{6}$$

where the $SSM < 0$ represents *SSM* for brighter regions and the $SSM > 0$ represents *SSM* for darker regions. t_s is the number of iterations (diffusion time). For the binary images without any noise, the proposed diffusion can be terminated automatically when the maximum intensity value becomes less than one (or less than another threshold such as 0.95). For the noisy images the selection of t_s depends on user and it is determined due to the noise level in the image. The overall process is completed by non-maxima suppression to make *SSM* thin, and hysteresis thresholding to observe binary skeleton.

3 Experimental Results and Discussions

We first present the comparison of the proposed diffusion with distance transform, Poisson equation and Gaussian filtering based techniques for medial function generation. The comparison is done on a flower shape object image of size 228×226, which is a pre-segmented binary image with perturbations on the boundary as shown in Figure 1 (a).

The distance transform [1] [10] [12] computes at each shape point its nearest distance to the shape boundary. The first column from the left in Figure 1 (b) shows the medial function generated by the distance transform on the flower shape object. The second column in Figure 1 (b) illustrates level-sets of the distance field. It is observed that the level-sets obtained by the distance transform, especially near the boundary, are not smooth and sensitive to the small perturbations of the boundary. The reason is, distance transform assign each value on

(a) Flower shape object image of size 228×226 with perturbations on the boundary

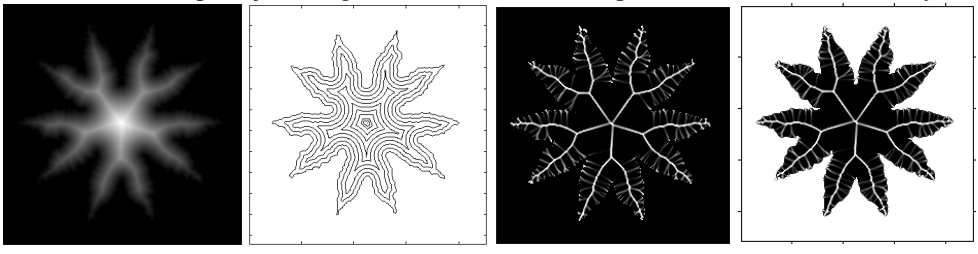

(b) Distance transform [1] [10] [14]

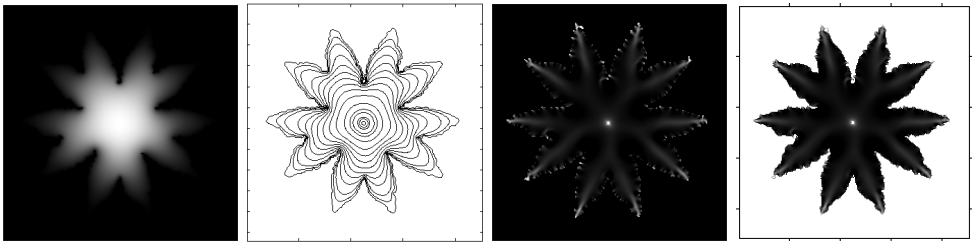

(c) Poisson equation (Linear diffusion) [6]

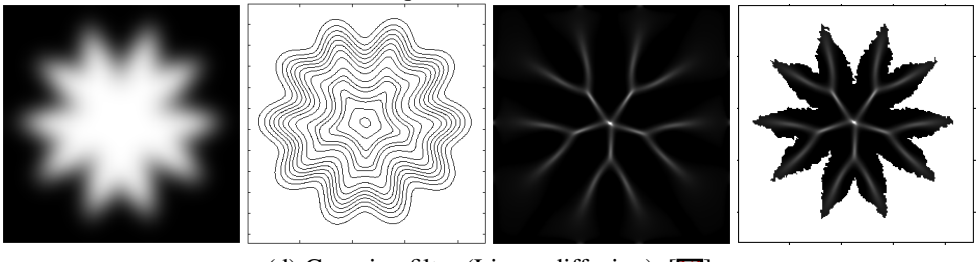

(d) Gaussian filter (Linear diffusion) [13]

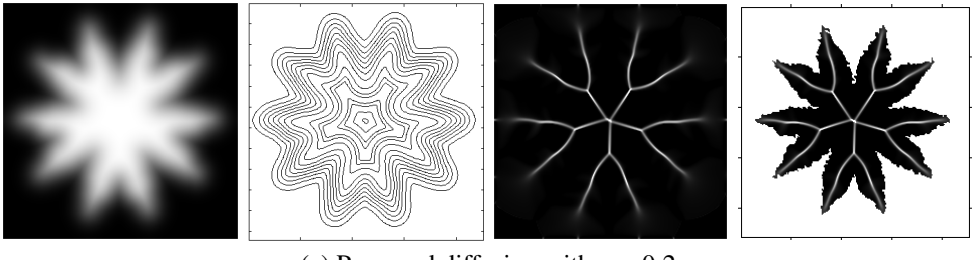

(e) Proposed diffusion with $c = 0.2$

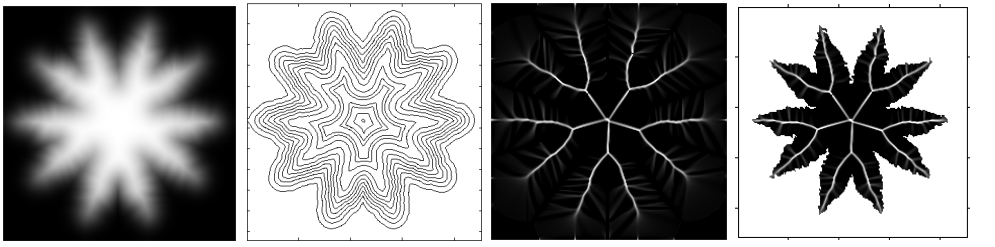

(f) Proposed diffusion with $c = 0$

Figure 1: Comparison of the proposed diffusion with distance transform, Poisson equation and Gaussian filter for medial function generation. The first column from the left is medial functions. The second column is level-sets. The third column is the negative values of the mean curvature measure of the level sets ($SSM < 0$) and the last column is the SSM<0 and the object in the same image.

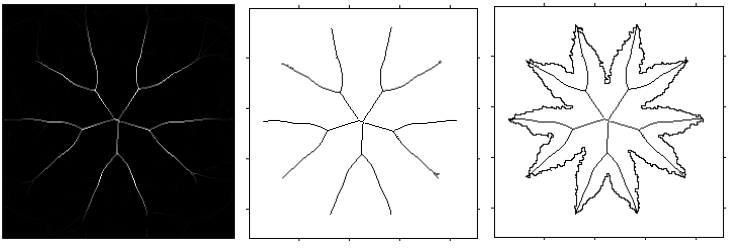

(a) (b) (c)

Figure 2: Obtaining thin and binary skeleton for $c = 0.2$. (a) Non-maxima suppressed skeleton strength map ($SSM < 0$), (b) Binary skeleton after hysteresis thresholding, (c) Skeleton with shape boundary.

shape according to the single boundary point (nearest one) and does not take into account other boundary points. The negative values of the mean curvature measure of the level-sets, which we use it to compute the SSM for brighter regions, can be used to show the quality of this surface for skeleton extraction. The $SSM < 0$ obtained by the distance transform is shown in the third column of Figure 1 (b). It can be seen that the $SSM < 0$ is affected by noisy boundary and it creates branches on the skeleton. The last column of the Figure 1 (b) also shows the $SSM < 0$ and the object in the same image. The distance transform is limited to pre-segmented binary images, since it depends on shape boundary.

The Poisson equation arises in gravitation and electrostatics. The Poisson equation problem [6], which has been introduced for shape representation and skeleton extraction, is a linear diffusion that has steady-state and unique solution. The first column from the left in Figure 1 (c) shows the medial function generated by the Poisson equation on the flower shape object. The second column in Figure 1 (c) shows the level-sets of the Poisson equation based medial function. It is observed that level-sets at the interior regions of the object are very smooth and the curvatures that can define the skeleton locations are almost lost. The level-sets close to the boundary of the object are also affected by the noise on the boundary. The $SSM < 0$ computed for the Poisson equation based medial function is shown in the third column of Figure 1 (c). The $SSM < 0$ is quite blurry at the interior regions and the skeleton features are lost. There are also noises close to the object boundary. Note that the application of the Poisson equation is limited to the pre-segmented binary images same as the distance transform, since it depends on shape boundary.

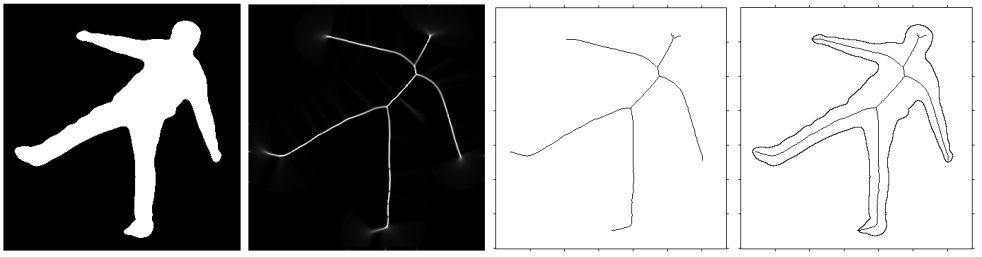

(a) Skeleton extraction without any noise in the binary image

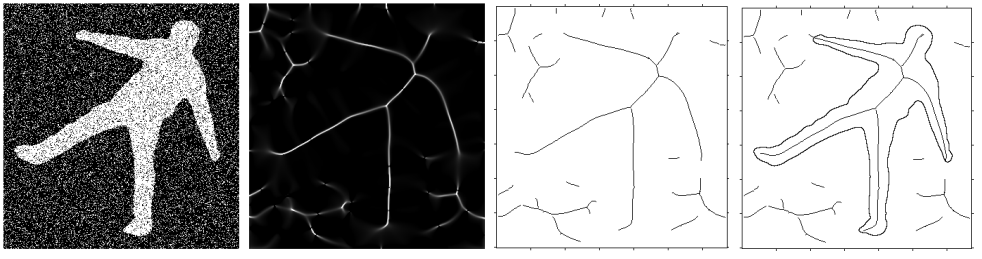

(b) Skeleton extraction with salt and pepper noise (density= 0.3)

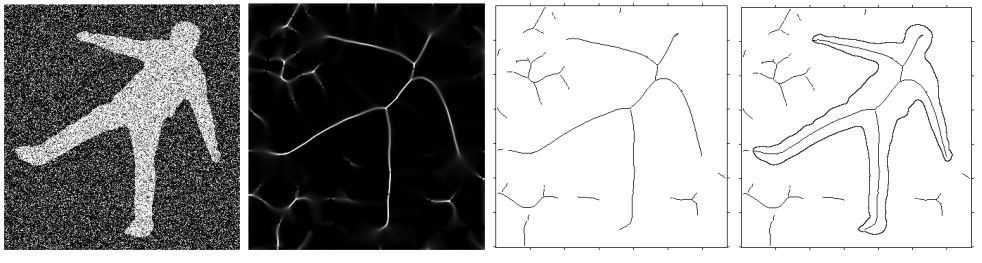

(c) Skeleton extraction with Gaussian noise (mean= 0, standard deviation= 0.4)

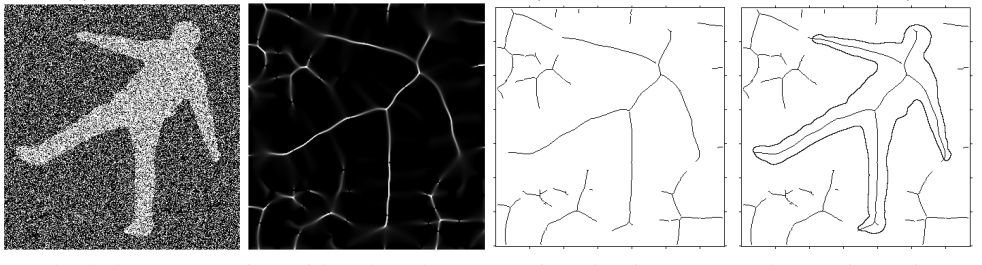

(d) Skeleton extraction with Salt and pepper noise (density= 0.3) and Gaussian noise (mean= 0, standard deviation= 0.4)

Figure 3: Experimentation with respect to noise in the binary image of size 350×335. The first column from the left is original images. The second column is the skeleton strength map for brighter regions $SSM < 0$. The third column is thin and binary skeleton and the last column is the binary skeleton with the subject shape in the same image.

Gaussian scale-space [13] is also used for skeletonization that can be applied to both binary and gray-scale images. Gaussian filtering can be equivalently viewed as the solution of linear heat diffusion equation, which is a direction and space invariant diffusion. Figure 1 (d) shows the medial function generated by the linear diffusion of the image after diffusion time $t_s = 250$. The second column in Figure 1 (d) illustrates level-sets of the medial function obtained after the linear diffusion. From the level-sets, it is observed that linear heat diffusion

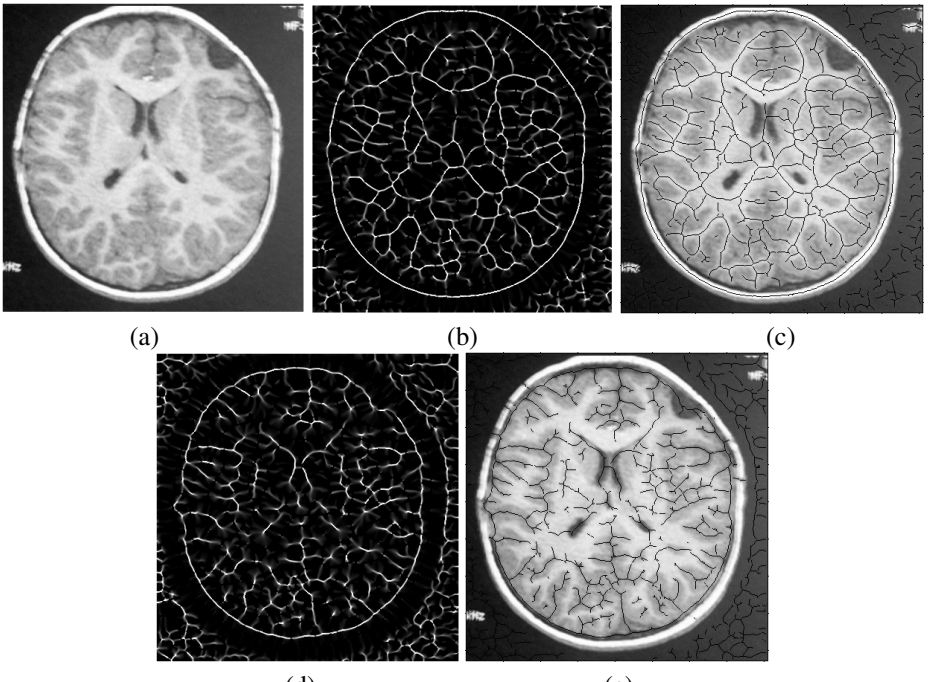

Figure 4: Skeletonization of gray-scale brain image of size 413×404. (a) The human brain, (b) Skeleton strength map for brighter regions ($SSM < 0$), (c) Binary skeleton for $SSM < 0$, (d) Skeleton strength map for darker regions ($SSM > 0$), (e) Binary skeleton for $SSM > 0$.

removes noise on the boundary. However, it also smoothes prominent curvatures of the shape and cause blurry skeleton features, which are almost lost as shown in the third column of Figure 1 (d) (the $SSM < 0$). If we increase the diffusion time, we will lose skeleton features more. On the other hand if we decrease diffusion time, the diffusion may not be enough to generate a medial function and to remove noise on the boundary.

Figure 1 (e) shows the proposed diffusion for skeleton extraction with $c = 0.2$. The first column from the left in Figure 1 (e) shows the medial function obtained by the proposed diffusion after $t_s = 250$, which is equal to the diffusion time in the linear heat flow in Figure 1 (d). The second column in Figure 1 (e) is the level-sets of the proposed medial function. It is observed that the proposed diffusion removes noise on the boundary and preserves prominent curvatures of the shape along the level sets, which represent skeleton features. The $SSM < 0$ is shown in the third column of Figure 1 (e). The $SSM < 0$ highlights skeleton points very well in comparison to the Poisson equation and Gaussian filter, which are linear diffusion based approaches. As well as, there is no noise close to the object boundary in comparison to the distance transform and Poisson equation. Figure 1 (f) also shows the proposed diffusion with parameter value $c = 0$ and diffusion time $t_s = 250$. From the level-sets, it is observed that prominent curvatures become sharper, while removing noise mostly. Choosing parameter value $c = 0.2$ provides smoother skeleton than $c = 0$, since small amount of tangential diffusion smoothes along the level sets.

Once we obtain the $SSM < 0$ with $c = 0.2$, which is shown in the third column of Figure 1 (e), the overall process is completed by non-maxima suppression to make skeleton thin and hysteresis thresholding to obtain binary skeleton as illustrated in Figure 2 (a) and (b),

respectively. Figure 2 (c) also shows the skeleton and shape of the object in the same image.

We experiment our algorithm with respect to noise in the image as well. Figure 3 (a) shows skeleton extraction in a binary image of the human of size 350×335 without any noise. In this experiment, $c = 0.2$ and the diffusion terminates automatically when the maximum intensity value in the image becomes less than one ($t_s = 231$). The first column from the left in Figure 3 (a) shows the original binary image without any noise. The second column in Figure 3 (a) is the $SSM < 0$. The third column in Figure 3 (a) illustrates the computed binary skeleton and the last column in Figure 3 (a) shows the binary skeleton and the shape of the subject in the same image. It is observed that the skeleton is extracted. Figure 3 (b) shows skeleton extraction in the same binary image after adding salt and pepper noise. The first column from the left in Figure 3 (b) shows the salt and pepper noise corrupted image with density= 0.3. The second column in Figure 3 (b) is the $SSM < 0$, which is computed after terminating diffusion at $t_s = 720$ and with $c = 0.2$. Here, t_s is determined by user and it has higher value since there are noises in the image. The third column is the binary skeleton and the last column in Figure 3 (b) illustrates the skeleton with the original shape of the subject. To visual inspection, the skeleton of the subject extracted in Figure 3 (b) is very similar to the skeleton extracted in Figure 3 (a). It is seen that the skeleton of the subject is detected without any dislocation and without missing any part of the subject. There are also some skeletons extracted at the background because of the noise. Figure 3 (c) shows the Gaussian noise corrupted image with mean= 0 and standard deviation= 0.4. It is observed that the skeleton of the subject is detected. Here, $c = 0.2$ and $t_s = 720$, which is same as the previous experiment in Figure 3 (b). There are also some skeletons detected at the background because of the noise. The skeleton of the subject is again very similar to the skeleton detected in Figure 3 (a) and (b). Finally, Figure 3 (d) illustrates skeletonization of the noisy image, which is corrupted by both Gaussian noise (mean= 0 and standard deviation= 0.4) and salt and pepper noise (density= 0.3). In this experiment, the input image has very poor quality as shown in the first column of the Figure 3 (d). The parameter values, $c = 0.2$ and $t_s = 720$, are same as the previous experiments in Figure 3 (b) and (c). It is seen that the skeleton of the subject is extracted with small perturbations. There are also some skeletons detected at the background because of the noise.

Experimental results also show that our algorithm can extract skeletons in gray-scale images. Figure 4 (a) shows a human brain image of size 413×404 . Figure 4 (b) shows the $SSM < 0$ that is computed after proposed anisotropic diffusion with parameter values $c = 0.2$ and $t_s = 60$. The $SSM < 0$ represents the skeleton strength map of the brighter regions in the image. The binary skeleton computed from the $SSM < 0$ is shown in Figure 4 (c). The $SSM > 0$ that represents the skeleton strength map of the darker regions is shown in Figure 4 (d). The binary skeleton obtained from the $SSM > 0$ is illustrated in Figure 4 (e). It is observed that skeletons of the brighter and the darker regions are detected.

4 Conclusions and Future Work

We have presented a novel skeleton extraction algorithm based on anisotropic heat flow analogy. A high quality medial function is computed with the proposed anisotropic diffusion. Then, the skeleton strength map (SSM) is defined with mean curvature measure. Finally, non-maxima suppression and hysteresis thresholding is applied to obtain thin and binary skeleton. The proposed anisotropic diffusion provides high quality skeleton features, while denoising the image and the object boundary. Results indicate that proposed diffusion generates better

medial function than distance transform, Poisson equation (linear diffusion) and Gaussian filtering (linear diffusion). Results also show that our technique can be applied to both binary and gray-scale images. In future work, we will inroduce a mechanism for automatic selection of diffusion time (number of iterations) for skeleton extraction purpose. In addition, the proposed diffusion will be extended to 3D for curve skeleton extraction.

5 Acknowledgements

This work is supported by an Innovation Partnership between Sony-Toshiba-IBM and Enterprise Ireland (IP-2007-505) and forms part of Trinity's Sony-Toshiba-IBM European Cell/B.E. Center of Compedence.

References

[1] C. Arcelli and G. S. Baja. Ridge points in euclidean distance maps. *Pattern Recognition Letters*, 13:237–243, 1992.

[2] H. Blum. A transformation for extracting new descriptors of shape. *Models for the Perception of Speech and Visual Form*, pages 363–380, 1967.

[3] F. Le Bourgeois and H. Emptoz. Skeletonization by gradient diffusion and regularization. In *Proc. IEEE Int'l. Conf. Image Processing*, volume 3, pages 33–36, 2007.

[4] C. Direkoglu. Feature extraction via heat flow analogy. phd thesis, university of southampton. 2009.

[5] C. Direkoglu and M. S. Nixon. Shape extraction via heat flow analogy. In *Proc. Int'l. Conf. Advanced Concepts for Intelligent Vision Systems*, volume 4678, pages 553–564, 2007.

[6] L. Gorelick, M. Galun, and A. Brandt. Shape representation and classification using the poisson equation. *IEEE Transactions on Pattern Analysis and Machine Intelligence*, 28 (12):1991–2005, 2006.

[7] T. Grogorishin, G. Abdel-Hamid, and Y. H. Yang. Skeletonization: An electrostatic field-based approach. *Pattern Analysis and Application*, 1(3):163–177, 1996.

[8] R. Hummel. Representations based on zero-crossings in scale-space. In *Proc. IEEE Int'l. Conf. Computer vision and Pattern Recognition*, pages 204–209, 1986.

[9] B. B. Kimia and K. Siddiqi. Geometric heat equation and nonlinear diffusion of shapes and images. In *Proc. IEEE Int'l. Computer Vision and Pattern Recognition*, pages 113–120, 1994.

[10] R. Kimmel, D. Shaked, N. Kiryati, and A. M. Bruckstein. Skeletonization via distance maps and level sets. *Computer Vision and Image Understanding*, 62(3):382–391, 1995.

[11] J. Koenderink. The structure of images. *Biological Cybernetics*, 50:363–370, 1984.

[12] L. Lam, S. W. Lee, and C. Y. Suen. Thinning methodologies - a comprehensive survey. *IEEE Trans. on Pattern Analysis and Machine Intelligence*, 14(9):869–885, 1992.

[13] T. Lindeberg. Edge detection and ridge detection with automatic scale selection. *International Journal of Computer Vision*, 30(2):117–154, 1998.

[14] G. Malandain and S. F. Vidal. Euclidean skeletons. *Image and Vision Computing*, 16 (5):317–327, 1998.

[15] S. Manay and A. Yezzi. Anti-geometric diffusion for adaptive thresholding and fast segmentation. *IEEE Transactions on Image Processing*, 12(11):1310–1323, 2003.

[16] R. L. Ogniewicz and O. Kubler. Hierarchic voronoi skeletons. *Pattern Recognition*, 28 (3):343–359, 1995.

[17] K. Siddiqi, S. Bouix, A. Tannenbaum, and S. W. Zucker. The hamilton-jacobi skeleton. In *Proc. Int'l. Conf. Computer Vision*, pages 828–834, 1999.

[18] S. Tari, J. Shah, and H. Pien. Extraction of shape skeletons from gray-scale images. *Computer Vision and Image Understanding*, 66(2):133–146, 1997.

[19] T. Ursell. The diffusion equation - a multi-dimensional tutorial. http://www.rpgroup.caltech.edu/ natsirt/aph162/diffusion.pdf. 2007.

[20] A. Witkin. Scale-space filtering. In *Proc. Int'l. Joint Conf. Artificial Intelligence*, pages 1019–1021, 1983.

[21] C. Xu and J. L. Prince. Snakes, shapes and gradient vector flow. *IEEE Transactions on Image Processing*, 7(3):359–369, 1998.

[22] Z. Yu and C. Bajaj. A segmentation-free approach for skeletonization of gray-scale images via anisotropic vector diffusion. In *Proc. IEEE Int'l. Conf. Computer vision and Pattern Recognition*, pages 415–420, 2004.